Accumulation of c-Myc and proteasomes at the nucleoli of cells containing elevated c-Myc protein levels

Azadeh Arabi[1,2,*,‡], Cecilia Rustum[1,3,*], Einar Hallberg[1] and Anthony P. H. Wright[1,2]

[1]Natural Sciences Section, Södertörns University College, S-141 89 Huddinge, Sweden
[2]Department of Biosciences, Karolinska Institute, S-141 57 Huddinge, Sweden
[3]Department of Neurochemistry and Neurotoxicology, Stockholms University, S-106 91 Stockholm, Sweden
*These authors contributed equally to this work
‡Author for correspondence (e-mail: azadeh.arabi@sh.se)

Accepted 15 January 2003
Journal of Cell Science 116, 1707-1717 © 2003 The Company of Biologists Ltd
doi:10.1242/jcs.00370

Summary

c-Myc is a predominately nuclear transcription factor that is a substrate for rapid turnover by the proteasome system. Cancer-related mutations in c-Myc lead to defects in its degradation and thereby contribute to the increase in its cellular level that is associated with the disease. Little is known about the mechanisms that target c-Myc to the proteasomes. By using a GFP fusion protein and live analysis we show that c-Myc shuttles between the nucleus and cytoplasm and thus it could be degraded in either compartment. Strikingly, at elevated levels of expression c-Myc accumulates at nucleoli in some cells, consistent with saturation of a nucleolus-associated degradation system in these cells. This idea is further supported by the observation that proteasome inhibitor treatment causes accumulation of c-Myc at the nucleoli of essentially all cells. Under these conditions c-Myc is relatively stably associated with the nucleolus, as would be expected if the nucleolus functions as a sequestration/degradation site for excess c-Myc. Furthermore, during elevated c-Myc expression or proteasome inhibition, nucleoli that are associated with c-Myc also accumulate proteasomes. c-Myc and proteasomes co-localise in intranucleolar regions distinct from the dense fibrillar component of the nucleolus. Based on these results we propose a model for c-Myc downregulation where c-Myc is sequestered at the nucleoli. Sequestration of c-Myc is accompanied by recruitment of proteasomes and may lead to subsequent degradation.

Key words: Transcription factor, Proteasome inhibitor, Degradation, Stability, Photobleaching

Introduction

c-Myc is a transcriptional regulator and a key component in controlling cell growth (Dang et al., 1999; Henriksson and Luscher, 1996). Cellular levels of c-Myc are tightly regulated at multiple steps including transcription, translation and protein stability (Spencer and Groudine, 1991). A remarkable feature of c-Myc is its very short half-life of 20-30 minutes (Hann and Eisenman, 1984; Salghetti et al., 1999) and its rapid proteolysis by the Ubiquitin/26S proteasome pathway (Ciechanover et al., 1991; Flinn et al., 1998). Consistent with its central role in cellular proliferation deregulated levels of c-Myc are associated with many cancers (Marcu et al., 1992).

In addition to gene rearrangements and amplifications that cause elevated levels of c-Myc, mutations in the coding sequence are frequently found in human cancers (Axelson et al., 1995; Murphy et al., 1986). These mutations cluster in the N-terminal transactivation domain within or close to the evolutionarily conserved Myc-box I region with Thr58, a phosphorylation site, being a major hotspot. Characterisation of the N-terminal sequences, including the Myc box I and II region as elements responsible for c-Myc rapid proteolysis (Flinn et al., 1998; Salghetti et al., 1999), suggested that increased protein stability might be a consequence of these alterations. It was subsequently shown that these cancer-related mutations impair the rapid turnover of c-Myc by proteasomes and cause a substantially prolonged half life of the protein (Bahram et al., 2000; Gregory and Hann, 2000; Salghetti et al., 1999). Aberrant ubiquitin/proteasome-mediated degradation of c-Myc is therefore likely to play an important role in the pathogenesis of cancer. However, the mechanisms that target the regulated degradation of c-Myc via the proteasome remain unknown.

26S Proteasomes are multi-subunit proteases consisting of the 20S catalytic core and the 19S regulatory particle (DeMartino and Slaughter, 1999; Myung et al., 2001). Proteasomes have been detected both in the nucleus and the cytoplasm of mammalian cells (Brooks et al., 2000; Palmer et al., 1996), and photobleaching analysis of GFP-tagged proteasomes has revealed that they are highly mobile (Reits et al., 1997). Different models have emerged to explain how these proteases and their substrates come into contact. One is the ‘recruitment model’, according to which the function and distribution of proteasomes are regulated by the distribution of their substrates (Anton et al., 1999; Baumann et al., 2001). In contrast, other current models propose that the substrates of the proteasomes are translocated to cellular compartments containing appropriate proteasomes. For example, nuclear proteins such as the transcriptional regulators p53 and the

Arylhydrocarbon receptor are presumed to be substrates for cytoplasmic proteasomes (Davarinos and Pollenz, 1999; Freedman and Levine, 1998) since nuclear export via the Leptomycin-B-sensitive CRM1 system has been shown to be a necessary step in regulating the degradation of these proteins. In addition, there is evidence for proteasome-mediated protein degradation within the nucleus (Floyd et al., 2001). One of the nuclear structures associated with proteasomal degradation is the ND10 bodies (also called POD or PML-bodies) (Anton et al., 1999). Interestingly, the list of the proteins interacting and/or co-localising with these nuclear foci is growing and includes transcription regulators as well as proteasomes (Matera, 1999; Reyes, 2001).

In spite of the previous identification of regions within the c-Myc protein that contribute to its rapid degradation as well as their demonstrated importance for the oncogenic potential of c-Myc, we still have no knowledge about the mechanisms that target regulated c-Myc degradation. In this work we show that even though c-Myc is predominantly nuclear, it is potentially available for degradation in both the nucleus and the cytoplasm since the protein shuttles between these compartments. Furthermore, increased c-Myc levels, resulting form ectopic expression or proteasome inhibition, are associated with accumulation of the protein at the nucleoli. Nucleolus-associated c-Myc is relatively stably associated with regions distinct from the fibrillarin containing structures in nucleoli that also accumulate proteasomes concurrent with c-Myc accumulation. These results are consistent with a model in which excess c-Myc is sequestered and subsequently degraded in the nucleoli of mammalian cells.

Materials and Methods

Cell culture conditions

COS-7 (African green monkey kidney) cells were grown at 37°C with 5% CO_2, in DMEM supplemented with 10% FBS and 50 μg/ml Gentamycin. Proteasome inhibitors were added to the culture medium 3-8 hours prior to the experiments. Mock samples and DMSO-treated cells were cultured in parallel as controls. Stock solutions of the proteasome inhibitors were prepared in DMSO and used at the following final concentrations: 100 μM *N*-acetyl-Leu-Leu-Nle-CHO (ALLN) (Sigma), 50 μM Z-Leu-leu-leu-CHO (MG132) (Biomol Research laboratories), 10 μM Epoxomycin (Affiniti Research Products, UK).

Transfections

c-myc-GFP encoding the full-length human c-Myc protein fused to GFP at its C-terminal, has been used previously for functional studies of c-Myc (Satou et al., 2001; Yin et al., 2001). We are grateful to H. Ariga, Hokkaido University, for providing us this plasmid. In experiments with c-Myc-GFP the cells were transiently transfected with 1 μg (or an otherwise indicated amount) of the c-Myc-GFP expression vector using Effectene transfection kit (Qiagen, Kebo Lab, Stockholm) according to the manufacturer's protocol. Proteasome inhibitors were added to the culture medium 24 hours post transfection.

Cells were transfected with 1, 2 or 4 μg of the c-Myc-GFP expression vector. The total amount of DNA in each transfection was kept constant at a total of 4 μg by adding complementary amounts of the empty vector. The efficiency of the transfection, with the expression vector was determined by scoring the number of c-Myc-GFP-expressing cells. The values were 20%, 35% and 40% in cells transfected with 1, 2 and 4 μg, respectively. A total of 5000 cells in three independent transfections were analysed.

Western blotting

Whole-cell extracts were made as described previously (Flinn et al., 1998). Lysates were subjected to polyacrylamide SDS-PAGE. Proteins were elecrtophoretically transferred to Hybond C-super membrane (Amersham), and detected by immunostaining and chemoluminescence.

Immunofluorescence staining and microscopy

Cells grown on glass cover slips were fixed in 3.7% paraformaldehyde in PBS for 20 minutes, permeabilised in 0.5% Triton X-100 in PBS for 5 minutes. All steps were performed on ice. The cells were blocked with 2% BSA in PBS containing 0.1% Tween-20 for 1 hour, at room temperature or over night at 4°C. Cells were then incubated at room temperature with primary antibodies for 1 hour, washed four times in blocking buffer and then incubated at room temperature with fluorophore-conjugated secondary antibody for 1 hour. After incubating with the secondary antibody the cells were washed twice in 0.1% Tween-20 in PBS, before mounting.

Anti-c-Myc C33 (Santa Cruz Biotechnology, Santa Barbara, CA), anti-20S proteasome mAb PW 8265 (Affiniti Research Products), anti-20S proteasome 'core' rabbit pAb PW8155 (Affiniti Research Products), and Anit-Fibrillarin mAb (Cytoskeleton Inc., Denver) were used. Purified 20S proteasomes (mammalian), PW8720, was purchased from Affiniti Research Products.

Images were acquired using a Leica DM IRBE fluorescence microscope or a Leica TCS-SP confocal laser scanning microscope (Leica, Heidelberg, Germany). For the Leica DM IRBE fluorescence microscope a C4742-95 Hamamatsu CCD camera (Hamamatsu Photonics, Sweden) was used. The FITC/GFP fluorescence was analysed using a BP 470/40 nm excitation and a BP 525/50 nm (Dic 500 nm) emission filter combination. The TRITC fluorescence was analysed using a BP 546/14 nm excitation and a LP 590 nm (Dic 580 nm) emission filter combination. For the Leica TCS-SP laser scanning confocal microscope a 488 nm laser line from an Argon laser (20 mW) and a 568 nm laser line from a Krypton laser (20 mW) were used. The images were acquired by using a wavelength interval between 500-550 nm and 600-650 nm, respectively.

Live cell imaging and photobleaching experiments

A Leica TCS-SP laser scanning confocal microscope with a 488 nm laser line from an Argon laser (20 mW) was used to perform all live cell and photobleaching experiments. The images were acquired by using a wavelength interval between 500-580 nm. In the time-lapse experiment, cells were followed for 3 hours after proteasome inhibitor addition. Images were acquired every 120 seconds.

In fluorescence recovery after photobleaching (FRAP) experiments (Lippincott-Schwartz et al., 2001; Pederson, 2001), a defined region of cells was exposed to 100% laser intensity for 0.5-1 seconds. The fluorescence recovery was calculated from images acquired. For quantitative analysis the post-bleach intensities were normalised to correct for total loss of fluorescence due to photobleaching. The relative fluorescence intensity (RFI) was calculated as $RFI=(I_{B,t}/I_{N,t})\times100$, where $I_{B,t}$ is the fluorescence intensity of the bleached area at each time point and $I_{N,t}$ is the intensity of the unbleached area at the corresponding time points.

The mobile fraction (MF) from the FRAP experiment was calculated as $MF=(I_i-I_0)/(I_i-I_0)$, where I_i is the fluorescence intensity in the bleached region after full recovery, I_i is the fluorescence intensity before bleaching and I_0 is the fluorescence intensity just after bleaching.

In fluorescence loss in photobleaching (FLIP) experiments, cells expressing c-Myc-GFP were repeatedly bleached in a defined region with 100% laser intensity for 1 second. The cell was then imaged between the bleach pulses. The relative fluorescence intensity (RFI)

was calculated as $RFI=I_{B,t}/I_{B,0} \times 100$, where $I_{B,t}$ is the fluorescence intensity of region of interest (ROI), at each time point and $I_{B,0}$ is the intensity of the ROI before bleaching.

Results

c-Myc is highly mobile within the nucleus and shuttles between nucleus and cytoplasm

We have investigated the cellular distribution of c-Myc in COS-7 cells by indirect immunofluorescence microscopy and cell imaging, using a c-Myc-GFP fusion protein. Under normal growth conditions, the majority of endogenous c-Myc was evenly distributed in the nucleoplasm, but it was not detected in the nucleoli (Fig. 1A). A very weak cytoplasmic staining was also seen. To assess the localisation of the GFP-fused protein COS-7 cells were transiently transfected with a plasmid expressing a GFP-tagged c-Myc. The staining pattern for c-Myc-GFP was indistinguishable from that of endogenous c-Myc (Fig. 1A).

To study the mobility of c-Myc-GFP in the nucleoplasm we performed FRAP (fluorescence recovery after photobleaching) analysis. A defined area in the nucleus was bleached for 1 second. The cell was then imaged immediately after bleaching and then sequentially every second, to measure the recovery rate of the fluorescence signal. Fluorescence in the bleached spot recovered too quickly for determination of fluorescence recovery using our instrumentation (data not shown), demonstrating that c-Myc diffuses very rapidly within the nucleoplasm.

To determine whether the mobility of the nuclear c-Myc protein is restricted to the nuclear compartment we used FLIP (fluorescence loss in photobleaching). Cells expressing c-Myc-GFP were repeatedly bleached in a defined area of the cytoplasm. A series of time-lapse images of the cells were obtained showing the fluorescence signal before bleaching and after every bleach pulse. Repeated bleaching in the cytoplasm caused fading of the nuclear signal, indicating that nuclear c-Myc-GFP shuttles to the cytoplasm (Fig. 1B). The reduction in nuclear fluorescence was specific because no reduction was seen in the nucleus of an adjacent cell. Fig. 1C shows that substantial quenching of the fluorescence was observed within the order of minutes, indicating a relatively rapid rate of nuclear cytoplasmic exchange. Thus we conclude that the observed, steady state distribution of c-Myc results from a dynamic equilibrium in which c-Myc molecules move rapidly within the nucleoplasm and continuously shuttle between the nucleus and the cytoplasm.

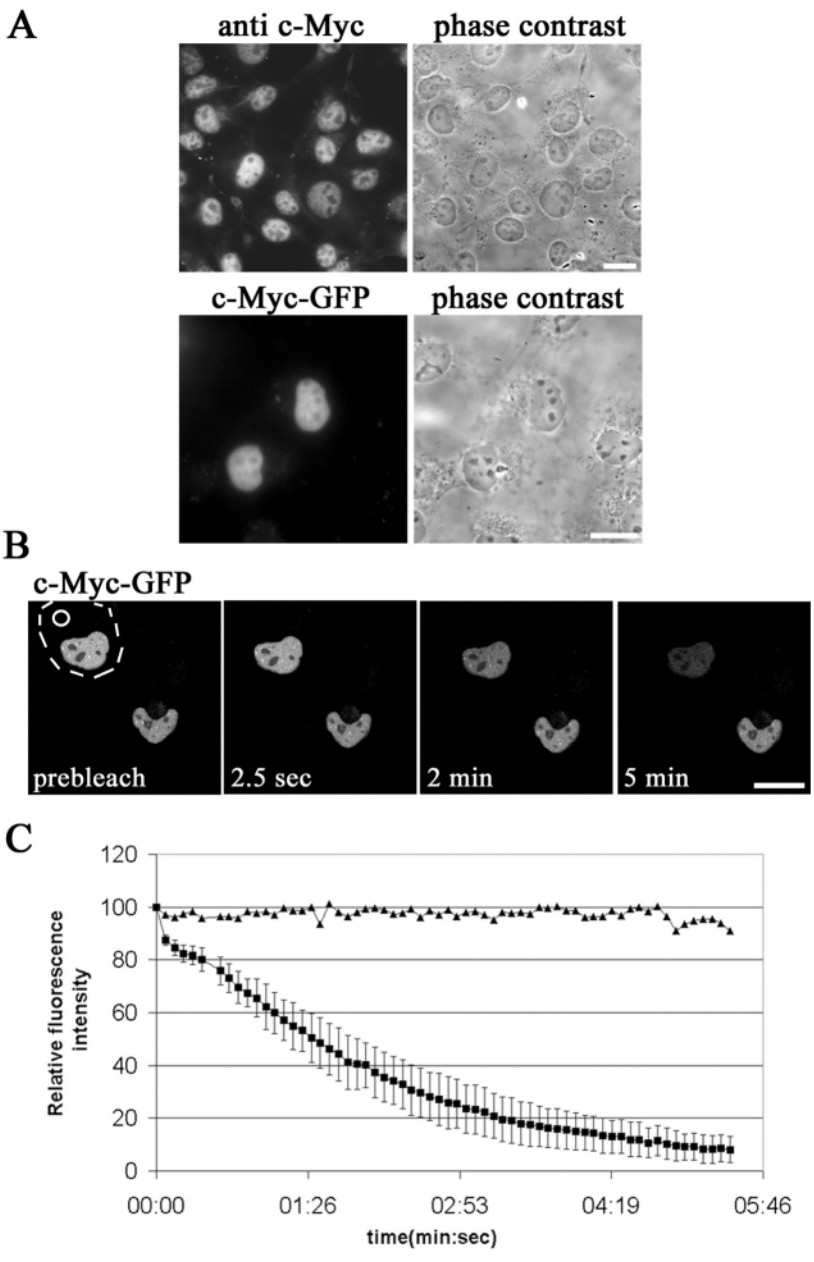

Fig. 1. Cellular distribution and nucleo-cytoplasmic shuttling of c-Myc. (A) c-Myc and c-Myc-GFP are predominantly nucleoplasmic. Both endogenous c-Myc (upper panels) and transiently transfected c-Myc-GFP (lower panels) were evenly distributed in the nucleoplasm while little or none was detected in the nucleoli of COS-7 cells. The cells (lower panel) were transfected with 1 μg of c-Myc-GFP expression plasmid. Bars, 20 μm. (B) FLIP analysis demonstrates that c-Myc-GFP shuttles between the nucleus and the cytoplasm. A COS-7 cell expressing c-Myc-GFP (outlined by the white dashed line) was repeatedly bleached, in a defined area in the cytoplasm (white circle). Confocal images were acquired before bleaching (pre-bleach) and between the bleach pulses. Images of the cell at the indicated times are shown. The lower cell, which was not bleached, serves as a control for unintentional bleaching during scanning. Bar, 20 μm.
(C) Comparison of fluorescence loss in bleached and unbleached cells. The fluorescence loss curve indicates the mean value for relative fluorescence intensity measured in the nucleoplasm of cells subjected to FLIP, plotted as a function of time (filled squares). The error bars show standard deviation (n=5 cells). The filled triangles indicate the relative fluorescent intensity in the nucleoplasm of the neighbouring unbleached cell shown in B.

Nucleolar association of c-Myc correlates with elevated levels of its expression

c-Myc was not observed in the nucleoli of most cells under normal growth conditions (Fig. 1A). However, careful inspection of endogenous c-Myc in COS-7 cells revealed that a very small portion of cells (<1%) accumulated c-Myc at the nucleoli. Similarly, we detected nucleolus-associated c-Myc-GFP in less than 1% of the transfected cells in our initial experiments (Fig. 1B).

To assess whether c-Myc expression levels could influence its nucleolar localisation, we progressively increased the levels of c-Myc-GFP expression by transfecting cells with increasing amounts of the expression plasmid. As expected, observation of the transfected cells showed that both the proportion of cells transfected, and the amount of expressed c-Myc-GFP in individual cells increase by increasing the amount of transfected vector. Interestingly, the proportion of cells containing c-Myc-GFP at the nucleoli (Fig. 2A, lower panels, yellow arrows), compared with cells containing nucleoplasmic c-Myc-GFP (Fig. 2A, upper panels), increased from <1% in cells transfected with 1 μg, to 4% and 8% in cells transfected with 2 and 4 μg, respectively (Fig. 2B).

Thus, although c-Myc is normally not detectable at the nucleoli, a small fraction of cells accumulate the protein in the nucleoli under physiological conditions of growth. The fraction of cells with nucleolar c-Myc-GFP increases progressively, as c-Myc expression levels increase. This suggests that the nucleolus might serve as a sequestration site for c-Myc when protein expression levels are high.

c-Myc accumulates at the nucleoli of cells treated with proteasome inhibitors

Since c-Myc levels increase in response to proteasome inhibitors (Salghetti et al., 1999), we investigated the cellular location of c-Myc in cells treated with proteasome inhibitor. COS-7 cells were cultured in the presence of the proteasome inhibitor, ALLN (100 μM), for 4 hours prior to analysis by indirect immunofluorescence microscopy. Strikingly, after proteasome inhibition c-Myc accumulated at the nucleoli of essentially all cells (Fig. 3A), which suggests that nucleolar-association becomes a bottle-neck in c-Myc degradation. Similarly to the endogenous protein, transiently transfected c-Myc-GFP was localised to the nucleoli in proteasome-inhibitor-treated cells. Similar results were obtained using other proteasome inhibitors such as MG132 (50 μM) as shown in Fig. 3B, and Epoxomicin (10 μM) (data not shown).

Using time-lapse analysis of c-Myc-GFP in living cells, we followed the translocation of c-Myc-GFP to the nucleoli as a result of proteasome inhibition in live cells. Within 3 hours of proteasome inhibitor addition c-Myc-GFP started to accumulate at the nucleolar periphery (Fig. 3B). The western blot in Fig. 3C shows that c-Myc accumulation occurs in the same time frame as its relocation to nucleoli during proteasome inhibition. These results are consistent with the existence of a cellular mechanism that targets c-

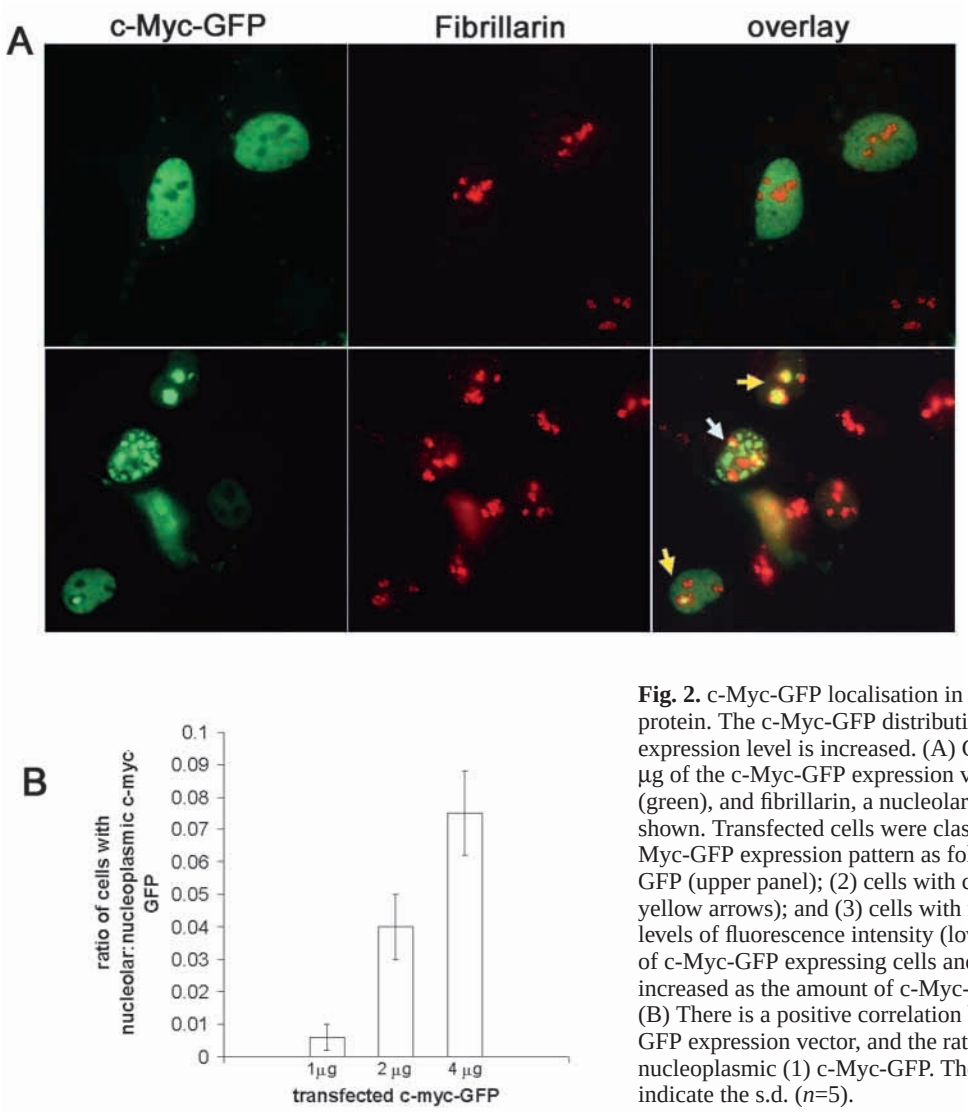

Fig. 2. c-Myc-GFP localisation in cells expressing elevated levels of the protein. The c-Myc-GFP distribution pattern changes progressively as its expression level is increased. (A) COS-7 cells were transfected with 1, 2 or 4 μg of the c-Myc-GFP expression vector. The distribution of c-Myc-GFP (green), and fibrillarin, a nucleolar marker (red), in representative cells is shown. Transfected cells were classified into three groups based on the c-Myc-GFP expression pattern as follows: (1) cells with nucleoplasmic c-Myc-GFP (upper panel); (2) cells with c-Myc-GFP in the nucleoli (lower panel, yellow arrows); and (3) cells with nuclear inclusions, which had the highest levels of fluorescence intensity (lower panel, grey arrow). The total number of c-Myc-GFP expressing cells and the number of cells in group 2 and 3 increased as the amount of c-Myc-GFP expression vector was increased. (B) There is a positive correlation between the amount of transfected c-Myc-GFP expression vector, and the ratio of cells with nucleolar (2): nucleoplasmic (1) c-Myc-GFP. The ratios are mean values. Error bars indicate the s.d. (*n*=5).

Myc to the nucleolus of cells containing elevated levels of the protein.

Using fibrillarin as a marker for the dense fibrillar region of the nucleolus, and 3D reconstitution of the confocal images we show at higher resolution that c-Myc is not detected in the nucleoli (Fig. 4A). In proteasome-inhibitor-treated cells c-Myc accumulates in regions distinct from the fibrillarin-containing regions of the nucleolus (Fig. 4B).

c-Myc is relatively stably associated with the nucleolus in cells treated with proteasome inhibitors

The data presented so far suggest that nucleoli might be a sequestration site for c-Myc. In order to determine whether nucleolus-associated c-Myc in these cells is still in equilibrium with other cellular compartments we performed FLIP analysis. As shown in Fig. 5A, in cells treated with 50 μM MG 132 for 3 hours, the fluorescence intensity of c-Myc-GFP in both the nucleoplasm and the nucleolus fades as a result of repeated bleaching in the cytoplasm, indicating that nucleolar c-Myc exchanges with the cytoplasmic pool of the protein. The residual mobility of nucleolar c-Myc further suggests that the accumulation of c-Myc cannot be attributed to the formation of a protein aggregate in the nucleoli.

To quantify the relative mobility of c-Myc accumulated at the nucleoli we used FRAP. c-Myc-GFP-expressing COS-7 cells were cultured in the presence of ALLN (100 μM) for 3 hours and then subjected to FRAP analysis. Cells with nucleolus-associated c-Myc-GFP were bleached within the nucleoli (Fig. 5B) or the nucleoplasm (data not shown), and then sequentially imaged to assess the recovery of the fluorescence signal. The fluorescence in the bleached nucleoli recovered within 30 minutes, with an average half-life of 6 minutes (Fig. 5C). The mobile fraction was calculated to 84%. The relatively slow fluorescence recovery kinetics of nucleolus-associated c-Myc-GFP compared with the recovery of the nucleoplasmic c-Myc-GFP is indicative of a relatively stable biological interaction between c-Myc-GFP and the nucleoli. As shown for untreated cells, the repopulation of c-Myc-GFP after bleaching in the nucleoplasm was too fast to measure in this experiment, indicating that the slower mobility of nucleolus-associated c-Myc is not just a general consequence of proteasome inhibition. Thus, although nucleolus-associated c-Myc is less mobile than nucleoplasmic c-Myc it is still dynamic and continues to shuttle to the cytoplasm. The reduced mobility of c-Myc associated with nucleoli compared with its mobility in the nucleoplasm shows that nucleoli provide sequestration sites for c-Myc when the protein is in excess.

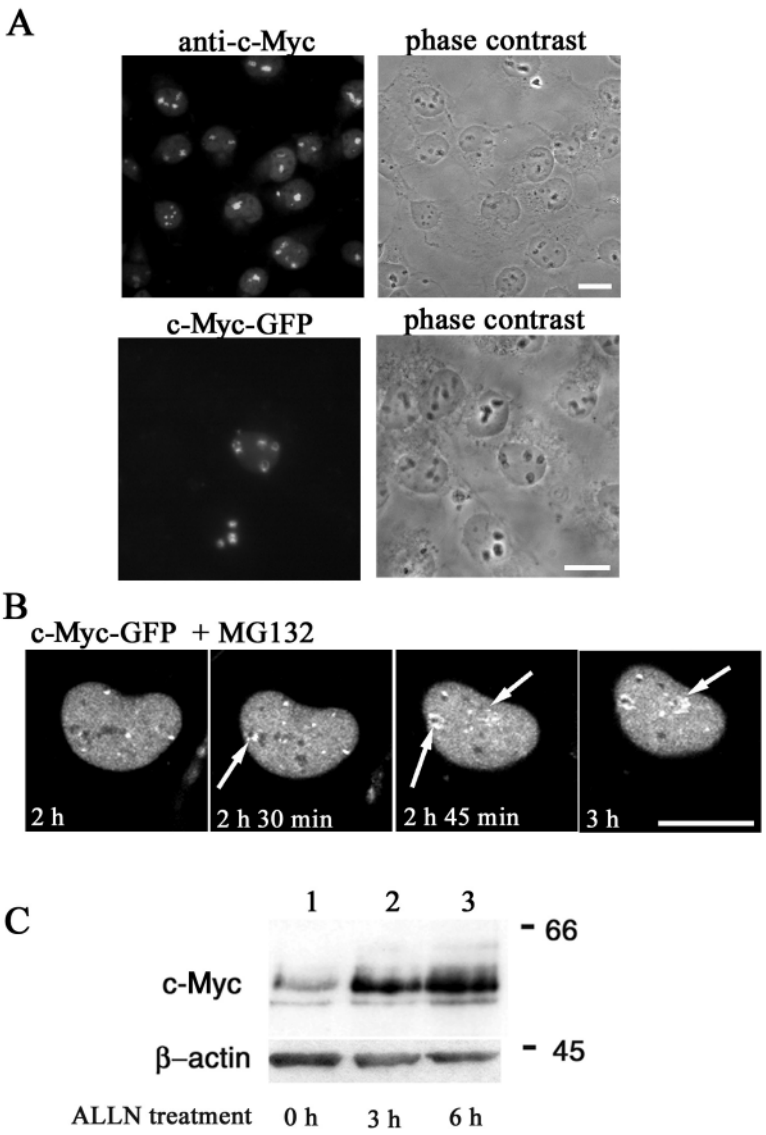

Fig. 3. Distribution of c-Myc in proteasome-inhibitor-treated cells. (A) c-Myc and c-Myc-GFP are nucleolar in proteasome-inhibitor-treated cells. COS-7 cells were cultured in the presence of 100 μM ALLN for 5 hours. Both c-Myc (upper panels) and c-Myc-GFP (lower panels) were localised to the nucleoli. The cells (lower panel) were transfected with 1 μg of c-Myc-GFP expression plasmid. Bar, 20 μm. (B) Time-lapse analysis shows redistribution of c-Myc-GFP in live cells after addition of 50 μM MG132. Confocal images were acquired every 120 seconds over a 3 hour period. The panel shows pictures selected at the times indicated. The arrows indicate accumulation of c-Myc-GFP in the vicinity of nucleoli. Nucleoli were identified by phase contrast microscopy as in A. Bar, 20 μm. (C) Proteasome inhibitor induced c-Myc redistribution is concurrent with its cellular accumulation. Whole cell extracts from COS-7 cells were analysed by SDS-PAGE and immunoblotting using anti-Myc C33 antibody. Lane 1 shows untreated cells. c-Myc protein levels increase after 3 and 6 hours of 100 μM ALLN treatment, lanes 2 and 3, respectively. β-actin was used as an internal loading control.

Proteasomes co-localise with nucleolus-associated c-Myc

c-Myc accumulates and is sequestered at nucleoli when its cellular level is increased. A potential consequence of this sequestration is subsequent proteasomal degradation. Degradation of c-Myc at the nucleoli would, however, require the presence of proteasomes at this location. To address this issue we investigated the localisation of proteasomes in the absence and the presence of proteasome inhibitors in COS-7

cells by immunofluorescence, using one monoclonal and one polyclonal antibody, both of which react with the core subunits of the proteasomes. In cells growing under normal conditions, proteasomes were localised in the nucleus and cytoplasm but could not be detected in nucleoli (Fig. 6A, upper panel). However, within 5 hours of proteasome inhibition a fraction of the proteasomes accumulated in the nucleoli, as shown by both antibodies (Fig. 6A, lower panel). Accumulation of the proteasomes in the nucleoli of proteasome-inhibitor-treated cells is shown at higher magnification in Fig. 6B (left panels). Confocal images of proteasome-inhibitor-treated cells stained for fibrillarin and proteasomes show that, like c-Myc, proteasomes accumulate in regions adjacent to but distinct from the fibrillarin-containing structures of the nucleolus (Fig. 6B, right panels).

Further investigation of the localisation of proteasomes in relation to c-Myc shows that proteasomes co-localise with c-Myc in the nucleoli of proteasome-inhibitor-treated cells (Fig. 7A). We detected proteasomes in the nucleoli of cells expressing elevated levels of c-Myc, in the absence of proteasome inhibitors (Fig. 7B). Interestingly, in these cells proteasomes accumulate specifically in the subset of nucleoli, which accumulate c-Myc. This strongly suggests a specific coupling of proteasome translocation to the nucleoli and accumulation of nucleolus-associated c-Myc.

Discussion

Like many other transcription factors, the level and activity of the c-Myc protein is highly regulated in mammalian cells.

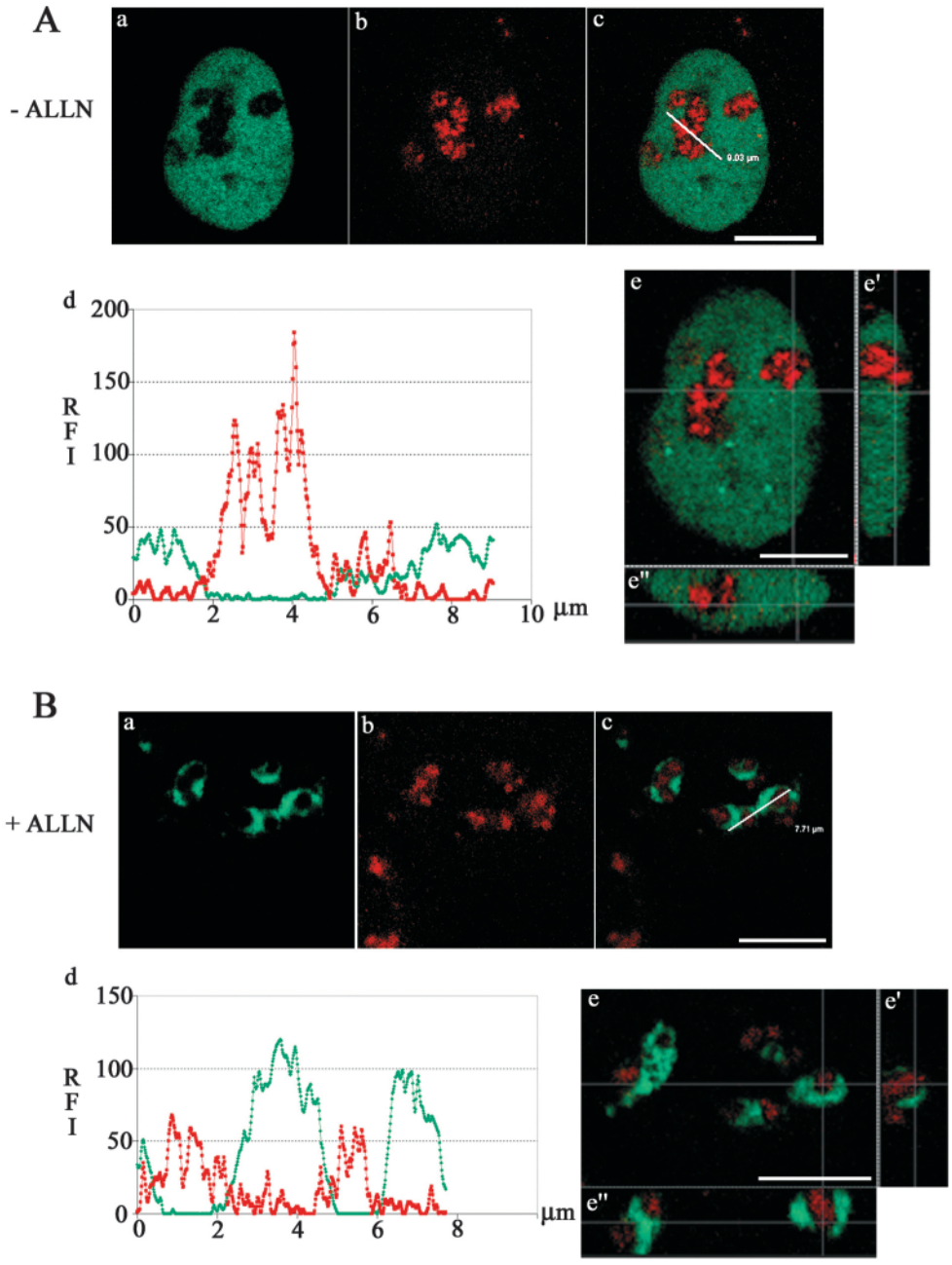

Fig. 4. Localisation of c-Myc in relation to fibrillarin. (A) c-Myc-GFP is predominantly located in the nucleoplasm of cells in the absence of proteasome inhibitors. Confocal images showing the distribution of c-Myc-GFP and fibrillarin in untreated COS-7 cells are shown in a and b, respectively. The distinct localisation of c-Myc-GFP and fibrillarin is shown in c-e. In c, the confocal images in a and b are overlaid. The relative fluorescence intensity (RFI) from c-Myc-GFP (green) and fibrillarin (red), along the white line in c is quantified in d. (e) Reconstitution of the stack of confocal xy plane images; e′ and e″ show yz and xz sections through the stack of images, respectively. The positions of the sections are shown by the fine white lines in e. Bar, 10 µm. (B) Nucleolus-associated c-Myc-GFP accumulates in regions adjacent to but distinct from the fibrillarin marker for the dense fibrillar region of the nucleolus in proteasome-inhibitor-treated cells. Confocal images showing the distribution of c-Myc-GFP and fibrillarin in cells treated with proteasome inhibitor are shown in a and b, respectively. The distinct localisation of c-Myc-GFP and fibrillarin within the nucleolus is shown in c-e. In c the confocal images in a and b are overlayed. The relative fluorescence intensity (RFI) from c-Myc-GFP (green) and fibrillarin (red), along the white line in c is quantified (d). (e) Reconstitution of the stack of confocal xy plane images; e′ and e″ show yz and xz sections through the stack of images, respectively. The positions of the sections are shown by the fine white lines in e. Bar, 10 µm.

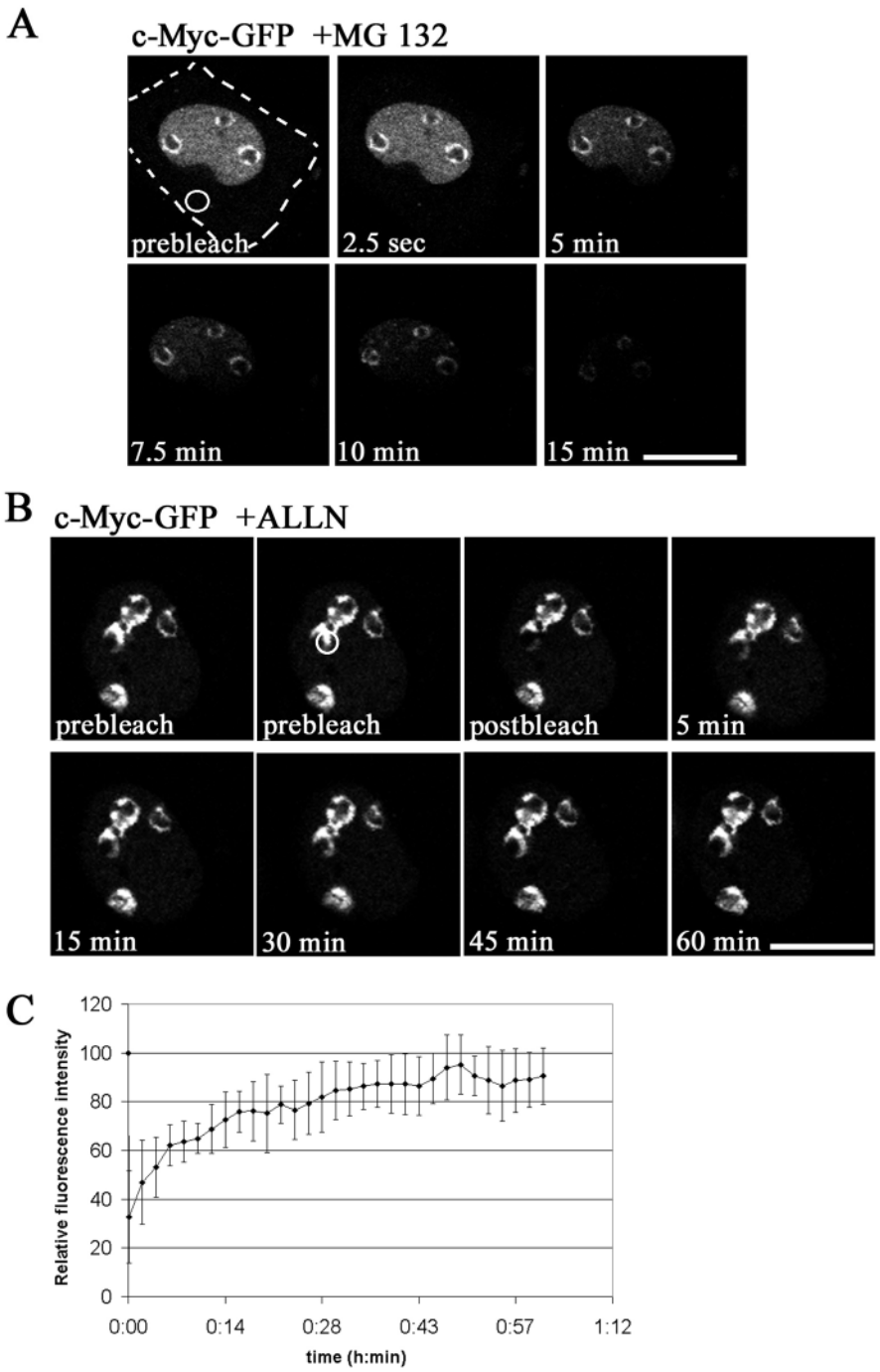

Fig. 5. Mobility of the nucleolar c-Myc-GFP in proteasome inhibitor treated cells. (A) FLIP analysis demonstrates that c-Myc-GFP shuttles between the nucleolus and the nucleoplasm/cytoplasm after proteasome inhibition. A cell expressing c-Myc-GFP (outlined by white dashed line) was treated with MG132 for 3 hours before being repeatedly bleached in a defined area in the cytoplasm (white circle). Confocal images of the cell were taken before bleaching and then at 2 second intervals. The panel shows images taken at the indicated time points. Bar, 20 μm. (B) FRAP analysis demonstrates a relatively stable interaction of c-Myc-GFP with a nucleolus after proteasome inhibition. A cell expressing c-Myc-GFP was treated with ALLN for 4 hours before being bleached in part of the nucleolus for 1 second (white circle). Confocal images were taken before bleaching and then every 120 seconds. The panel shows images taken at the indicated time points. Bar, 20 μm. (C) Quantitative measurements of the fluorescence recovery. The curve indicates the mean value for the relative fluorescence intensity plotted as a function of time. The error bars represent the standard deviation (n=5 cells). The fluorescence was recovered within 30 minutes and the mobile fraction was calculated to 84%.

Elevated levels of c-Myc protein have been reported to be significant for the development of cancer by deregulating gene activation (Marcu et al., 1992) and impairing the cellular proteolytic system (Gavioli et al., 2001). Here we show that elevation of c-Myc protein levels as a result of ectopic expression or defective breakdown due to proteasome inhibition, results in accumulation of the protein in the nucleoli of cells, a location in which it is found only rarely in normal cells. Our results suggest that nucleolar sequestration may be a new mechanism by which c-Myc activity is regulated and where defects might contribute to the ontology of cancer.

Accumulation of c-Myc in nuclear bodies or inclusions has been observed previously in transiently transfected cells overexpressing c-Myc (Henriksson et al., 1992; Koskinen et al., 1991). These inclusions are similar to the inclusions we also observe in cells, which appear to express the highest amounts of c-Myc-GFP (Fig. 2A, class 3 cells). Co-localisation of c-Myc with Hsp70 in such inclusions has led to speculation that they might be artefacts of the transfection procedure and formed by aggregates of unfolded c-Myc. However, as suggested by the same authors, it is equally possible that formation of these c-Myc/Hsp70-containing bodies may be a mechanism for regulating c-Myc activity (Henriksson et al., 1992; Koskinen et al., 1991). In support of this view it should be noted that c-Myc inclusions are also observed in non-transfected, cytokine-activated lymphocytes. (Heikkila et al., 1987; Larsson et al., 1991). Importantly, the nucleolar accumulation sites in our experiments are distinct from the nuclear bodies that have been observed previously since cells containing nucleolar c-Myc do not contain other sites of c-Myc accumulation (Figs 2-5).

A recent proteomic analysis of human nucleoli has shown that a surprisingly large number of proteins, many with no previously known nucleolar functions, are found in nucleoli (Andersen et al., 2002). This study reveals that the nucleolar protein composition is not static and can alter significantly in response to the metabolic state of the cell. Although conditions analogous to ours were not investigated in that study, the

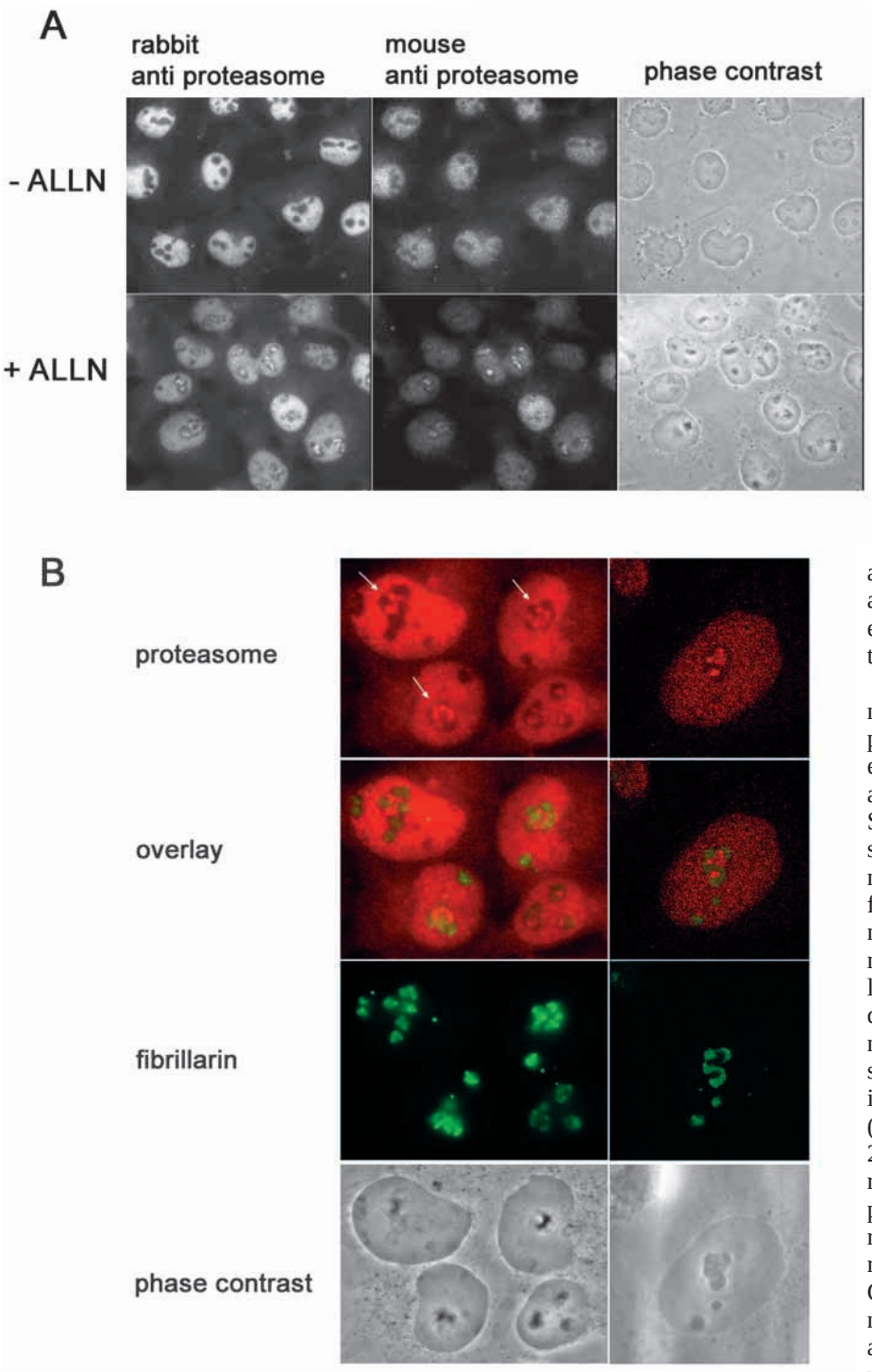

Fig. 6. Distribution of proteasomes in COS-7 cells in the presence and absence of proteasome inhibitors. (A) Proteasomes are recruited to the nucleolus in proteasome-inhibitor-treated cells. Cells were cultured in the presence or absence of 100 μM ALLN, and immunostained for proteasomes using a rabbit pAb (1:10,000) and a mouse mAb (1:500). Proteasomes were detected in the nucleus and the cytoplasm, but were not detected in the nucleoli of untreated cells (upper panels). In cells treated with ALLN for 5 hours, a subpopulation of proteasomes was detected in the nucleoli (lower panels). (B) Localisation of the proteasomes (red), and fibrillarin (green) in proteasome-inhibitor-treated cells is shown at higher magnification (left panels). Confocal images show the accumulation of proteasomes adjacent to the fibrillarin marker for the dense fibrillar region of the nucleolus in the nucleolus (right panels). Rabbit pAb was used for proteasomes immuno-staining.

findings are in general agreement with the idea that c-Myc and additional proteins translocate to the nucleoli under particular conditions such as proteasome inhibition or elevated expression. Interestingly, a number of proteins, including POD-associated proteins PML and sp100, SUMO-1 (Mattsson et al., 2001), EBNA-5 (Pokrovskaja et al., 2001) and MDM2 (Xirodimas et al., 2001) have been shown to localise to the nucleolus in response to proteasome inhibition. However, it has also been shown that some other proteins such as p27, p21 and cyclin D do not localise to the nucleolus under such conditions (Mattsson et al., 2001). Thus, it appears that the nucleolar association in response to proteasome inhibitors applies to only a subset of nuclear proteins and, to our knowledge, c-Myc is the first example of a transcription factor belonging to this class.

Regulation of protein activity by nucleolar sequestration has been reported previously (Tao and Levine, 1999; Visintin et al., 1999). It is thus likely that c-Myc activity can also be regulated in this way. Such a model would predict a relatively stable interaction of c-Myc with the nucleolus in order to remove it from the functional pool of c-Myc in the nucleoplasm. We used FRAP to measure the mobility of c-Myc in alternative nuclear locations. The results show that c-Myc diffuses very rapidly within the nucleoplasm. This is consistent with other studies of transcriptional regulators including HP1 (Kourmouli et al., 2000), GR (Hager et al., 2000) and ER (Stenoien et al., 2001). Based on these findings a ‘hit and run’ model for gene regulation has been proposed according to which transcriptional regulators are in continual flux and move rapidly in and out of the chromatin. Consistent with sequestration in the nucleolus, the mobility of c-Myc-GFP associated with the nucleolus is strikingly reduced compared with the rapid dynamics seen in the nucleoplasm. Although re-population of bleached nucleoli with actively fluorescent c-Myc-GFP molecules from the nucleoplasm or other nucleolar sources is slow, nucleolar c-Myc is still mobile. The rates of re-population are much faster than those observed for components of well-characterised stable structures, such as the nuclear pore complexes (Daigle et al., 2001). The relatively stable but still mobile nucleolar c-Myc pool shows that the

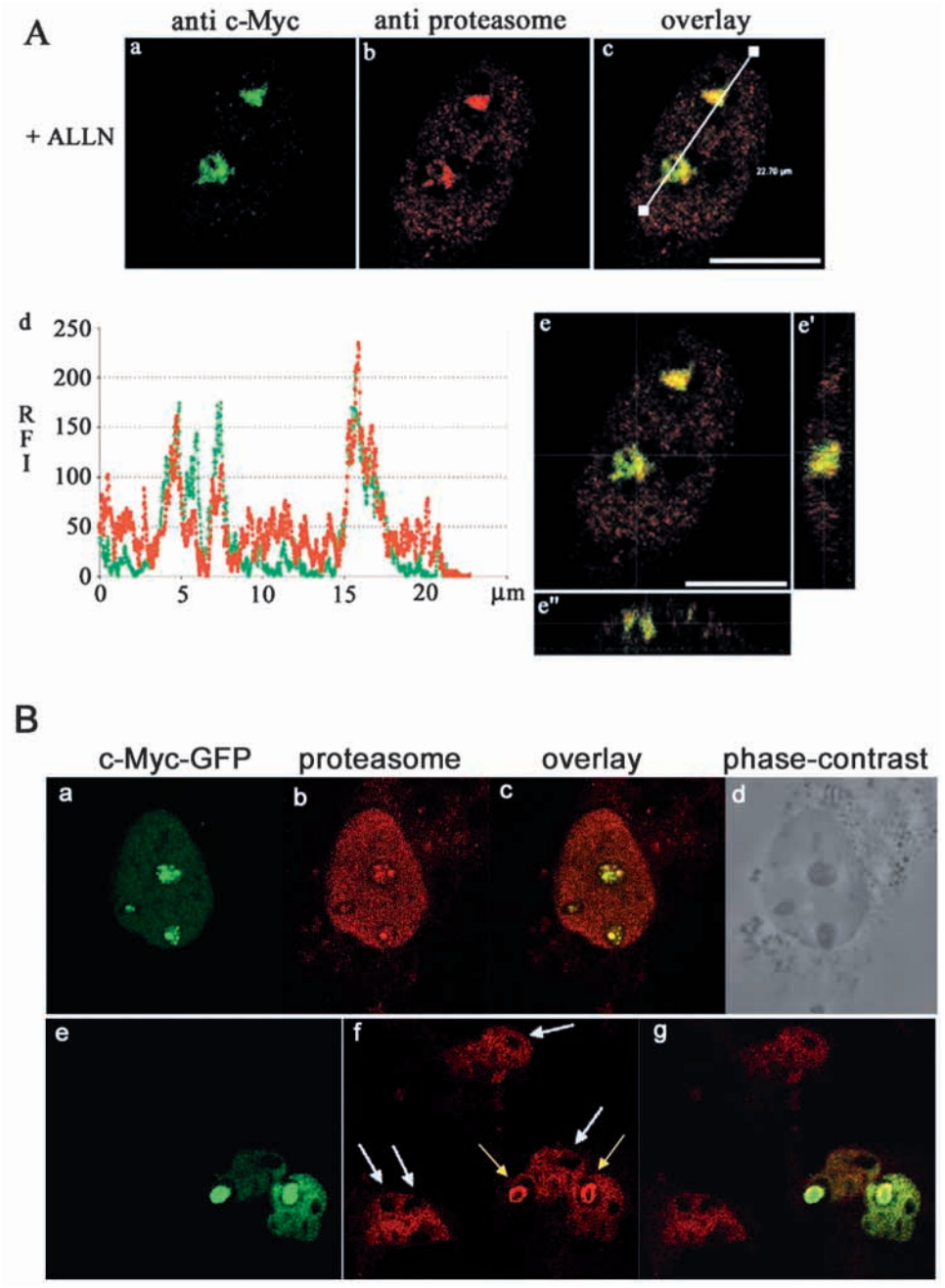

Fig. 7. Localisation of proteasomes in relation to c-Myc in proteasome inhibitor treated cells. (A) The distribution of c-Myc and proteasomes in a proteasome-inhibitor-treated cell is shown at high resolution by the confocal images in a and b, respectively. The colocalisation of c-Myc and proteasomes is shown in c-e. In c the confocal images in a and b are overlayed. The relative fluorescence intensity from c-Myc (green) and proteasomes (red), along the white line in c is quantified in d. (e) Reconstitution of the stack of confocal xy plane images; e′ and e″ show yz and xz sections through the stack of images, respectively. The positions of the sections are shown by the fine white lines in e. Bar, 10 µm. (B) The distribution of c-Myc-GFP and proteasomes in cells expressing increased levels of c-Myc in the absence of proteasome inhibitor is shown by the confocal images a-d. Proteasomes accumulate specifically in the nucleoli that contain c-Myc (e-g, yellow arrows). Nucleoli lacking c-Myc remain devoid of nucleolar proteasome staining (e-g, white arrowheads)

nucleolus fulfils the requirements for a nuclear sequestration site, from which the protein has the opportunity to re-enter the active c-Myc population in the nucleoplasm.

Our observation that proteasome inhibition causes c-Myc accumulation in the nucleoli of essentially all cells suggested that nucleolar sequestration of accumulating c-Myc might be augmented by inhibition of its degradation at nucleolar sites. Accordingly, our results demonstrate changes in proteasome localisation. We show that under normal growth conditions proteasomes are not detectable in nucleoli. In contrast, in response to proteasome inhibitors a fraction of the proteasomes accumulates in the nucleoli concurrent with the re-localisation of c-Myc. This is consistent with a recent report where proteasomes were shown to accumulate in the nucleoli of other mammalian cells following proteasome inhibition (Mattsson et al., 2001). Notably, redistribution of proteasomes to the nucleoli is not restricted to the conditions of proteasome inhibitor treatment since we show that, in cells expressing high levels of c-Myc in the absence of proteasome inhibitors, proteasomes are also associated with the subset of nucleoli that contain c-Myc.

There is independent evidence for alterations in proteasome distribution under experimental conditions similar to ours. Proteasome inhibitor treatment has been shown to promote accumulation of the proteasomes at the mitotic organising centre (MTOC) (Wigley et al., 1999; Wojcik et al., 1996). Moreover, studies with the mutant influenza virus nucleoprotein, which is a target of rapid proteasomal degradation, reveal that in the presence of proteasome inhibitors nucleoprotein accumulates in MTOC and PML bodies and recruits the proteasomes to both locations (Anton et al., 1999). When proteasome function is restored proteasomes degrade substrates in MTOC and PML bodies. One possible explanation to such alterations in proteasome localisation is that these enzymes might be able to seek out their targets at their accumulation/sequestration sites. Several lines of evidence support this view. Proteasome inhibitor treatment has been shown not to induce a general increase in

proteasome levels (Wigley et al., 1999), but rather the observed accumulation of proteasomes in specific regions appears to be caused by redistribution of the existing pools to the regions of substrate sequestration. Taken together with our data, these results support a model in which proteasomes are recruited to the nucleoli, where a subset of their substrates, including c-Myc, is sequestered. In most normal cells c-Myc would be rapidly degraded and this would be a simple way to explain the observation that c-Myc and proteasomes are not normally observed in the nucleoli.

The molecular chaperone protein Hsp70 has been shown to interact with the nuclear accumulations of c-Myc (Henriksson et al., 1992; Koskinen et al., 1991). In agreement with this we have observed that Hsp70 also co-localises with excess c-Myc, which is sequestered at the nucleoli (A.A. and A.P.H.W., unpublished). However, the outcome of Hsp70 interaction with accumulated c-Myc remains unclear. In addition to its role in regulating protein folding, Hsp70 interacts directly with the proteasomes via co-factors such as the CHIP (C-terminus of Hsp70-interacting protein) and BAG1 proteins (Alberti et al., 2002; Demand et al., 2001), which have been shown to regulate the proteasomal degradation of chaperone substrates. It is therefore tempting to speculate that Hsp70 might influence the fate of c-Myc sequestered at the nucleolus either by inducing c-Myc release or by targeting it for proteasomal degradation.

In summery, our results suggest that c-Myc activity is negatively regulated by both sequestration and proteasome-mediated degradation at the nucleoli. Our observation that c-Myc and proteasomes concurrently translocate to the nucleolus suggests that these mechanisms are coordinated and at least partly overlapping. Further studies will be required to determine the extent to which c-Myc sequestration is directly coupled to its degradation. It is possible that the extent of coupling may vary under different conditions of cell growth and proliferation.

We are especially grateful to H. Ariga (Hokkaido University) for supplying the c-Myc-GFP expression vector, and Lars Branden (Karolinska Institute) for his generous help and advice. This work was supported by the grants from Swedish Cancer Society (4273-B00-02XBB) (to A.P.H.W.). and grants from the Swedish Research Council for Engineering Sciences (TFR 1999-145) and Carl Tryggers stiftelse (to E.H.). A.P.H.W. is a Senior Investigator supported by the Swedish Science Research Council.

References

Alberti, S., Demand, J., Esser, C., Emmerich, N., Schild, H. and Hohfeld, J. (2002). Ubiquitylation of BAG-1 suggests a novel regulatory mechanism during the sorting of chaperone substrates to the proteasome. *J. Biol. Chem.* **277**, 45920-45927.

Andersen, J. S., Lyon, C. E., Fox, A. H., Leung, A. K., Lam, Y. W., Steen, H., Mann, M. and Lamond, A. I. (2002). Directed proteomic analysis of the human nucleolus. *Curr. Biol.* **12**, 1-11.

Anton, L. C., Schubert, U., Bacik, I., Princiotta, M. F., Wearsch, P. A., Gibbs, J., Day, P. M., Realini, C., Rechsteiner, M. C., Bennink, J. R. et al. (1999). Intracellular localization of proteasomal degradation of a viral antigen. *J. Cell Biol.* **146**, 113-124.

Axelson, H., Henriksson, M., Wang, Y., Magnusson, K. P. and Klein, G. (1995). The amino-terminal phosphorylation sites of C-MYC are frequently mutated in Burkitt's lymphoma lines but not in mouse plasmacytomas and rat immunocytomas. *Eur. J. Cancer* **31A**, 2099-2104.

Bahram, F., von der Lehr, N., Cetinkaya, C. and Larsson, L. G. (2000). c-Myc hot spot mutations in lymphomas result in inefficient ubiquitination and decreased proteasome-mediated turnover. *Blood* **95**, 2104-2110.

Baumann, C. T., Ma, H., Wolford, R., Reyes, J. C., Maruvada, P., Lim, C., Yen, P. M., Stallcup, M. R. and Hager, G. L. (2001). The glucocorticoid receptor interacting protein 1 (GRIP1) localizes in discrete nuclear foci that associate with ND10 bodies and are enriched in components of the 26S proteasome. *Mol. Endocrinol.* **15**, 485-500.

Brooks, P., Fuertes, G., Murray, R. Z., Bose, S., Knecht, E., Rechsteiner, M. C., Hendil, K. B., Tanaka, K., Dyson, J. and Rivett, J. (2000). Subcellular localization of proteasomes and their regulatory complexes in mammalian cells. *Biochem. J.* **346 Pt 1**, 155-161.

Ciechanover, A., DiGiuseppe, J. A., Bercovich, B., Orian, A., Richter, J. D., Schwartz, A. L. and Brodeur, G. M. (1991). Degradation of nuclear oncoproteins by the ubiquitin system in vitro. *Proc. Natl. Acad. Sci. USA* **88**, 139-143.

Daigle, N., Beaudouin, J., Hartnell, L., Imreh, G., Hallberg, E., Lippincott-Schwartz, J. and Ellenberg, J. (2001). Nuclear pore complexes form immobile networks and have a very low turnover in live mammalian cells. *J. Cell Biol.* **154**, 71-84.

Dang, C. V., Resar, L. M., Emison, E., Kim, S., Li, Q., Prescott, J. E., Wonsey, D. and Zeller, K. (1999). Function of the c-Myc oncogenic transcription factor. *Exp. Cell Res.* **253**, 63-77.

Davarinos, N. A. and Pollenz, R. S. (1999). Aryl hydrocarbon receptor imported into the nucleus following ligand binding is rapidly degraded via the cytosplasmic proteasome following nuclear export. *J. Biol. Chem.* **274**, 28708-28715.

Demand, J., Alberti, S., Patterson, C. and Hohfeld, J. (2001). Cooperation of a ubiquitin domain protein and an E3 ubiquitin ligase during chaperone/proteasome coupling. *Curr. Biol.* **11**, 1569-1577.

DeMartino, G. N. and Slaughter, C. A. (1999). The proteasome, a novel protease regulated by multiple mechanisms. *J. Biol. Chem.* **274**, 22123-22126.

Flinn, E. M., Busch, C. M. and Wright, A. P. (1998). myc boxes, which are conserved in myc family proteins, are signals for protein degradation via the proteasome. *Mol. Cell Biol.* **18**, 5961-5969.

Floyd, Z. E., Trausch-Azar, J. S., Reinstein, E., Ciechanover, A. and Schwartz, A. L. (2001). The nuclear ubiquitin-proteasome system degrades MyoD. *J. Biol. Chem.* **276**, 22468-22475.

Freedman, D. A. and Levine, A. J. (1998). Nuclear export is required for degradation of endogenous p53 by MDM2 and human papillomavirus E6. *Mol. Cell Biol.* **18**, 7288-7293.

Gavioli, R., Frisan, T., Vertuani, S., Bornkamm, G. W. and Masucci, M. G. (2001). c-myc overexpression activates alternative pathways for intracellular proteolysis in lymphoma cells. *Nat. Cell Biol.* **3**, 283-288.

Gregory, M. A. and Hann, S. R. (2000). c-Myc proteolysis by the ubiquitin-proteasome pathway: stabilization of c-Myc in Burkitt's lymphoma cells. *Mol. Cell Biol.* **20**, 2423-2435.

Hager, G. L., Fletcher, T. M., Xiao, N., Baumann, C. T., Muller, W. G. and McNally, J. G. (2000). Dynamics of gene targeting and chromatin remodelling by nuclear receptors. *Biochem. Soc. Trans.* **28**, 405-410.

Hann, S. R. and Eisenman, R. N. (1984). Proteins encoded by the human c-myc oncogene: differential expression in neoplastic cells. *Mol. Cell Biol.* **4**, 2486-2497.

Heikkila, R., Schwab, G., Wickstrom, E., Loke, S. L., Pluznik, D. H., Watt, R. and Neckers, L. M. (1987). A c-myc antisense oligodeoxynucleotide inhibits entry into S phase but not progress from G0 to G1. *Nature* **328**, 445-449.

Henriksson, M., Classon, M., Axelson, H., Klein, G. and Thyberg, J. (1992). Nuclear colocalization of c-myc protein and hsp70 in cells transfected with human wild-type and mutant c-myc genes. *Exp. Cell Res.* **203**, 383-394.

Henriksson, M. and Luscher, B. (1996). Proteins of the Myc network: essential regulators of cell growth and differentiation. *Adv. Cancer Res.* **68**, 109-182.

Koskinen, P. J., Sistonen, L., Evan, G., Morimoto, R. and Alitalo, K. (1991). Nuclear colocalization of cellular and viral myc proteins with HSP70 in myc-overexpressing cells. *J. Virol.* **65**, 842-851.

Kourmouli, N., Theodoropoulos, P. A., Dialynas, G., Bakou, A., Politou, A. S., Cowell, I. G., Singh, P. B. and Georgatos, S. D. (2000). Dynamic associations of heterochromatin protein 1 with the nuclear envelope. *EMBO J.* **19**, 6558-6568.

Larsson, L. G., Schena, M., Carlsson, M., Sallstrom, J. and Nilsson, K. (1991). Expression of the c-myc protein is down-regulated at the terminal stages during in vitro differentiation of B-type chronic lymphocytic leukemia cells. *Blood* **77**, 1025-1032.

Lippincott-Schwartz, J., Snapp, E. and Kenworthy, A. (2001). Studying protein dynamics in living cells. *Nat. Rev. Mol Cell Biol.* **2**, 444-456.

Marcu, K. B., Bossone, S. A. and Patel, A. J. (1992). myc function and regulation. *Annu. Rev. Biochem.* **61**, 809-860.

Matera, A. G. (1999). Nuclear bodies: multifaceted subdomains of the interchromatin space. *Trends Cell Biol.* **9**, 302-309.

Mattsson, K., Pokrovskaja, K., Kiss, C., Klein, G. and Szekely, L. (2001). Proteins associated with the promyelocytic leukemia gene product (PML)-containing nuclear body move to the nucleolus upon inhibition of proteasome-dependent protein degradation. *Proc. Natl. Acad. Sci. USA* **98**, 1012-1017.

Murphy, W., Sarid, J., Taub, R., Vasicek, T., Battey, J., Lenoir, G. and Leder, P. (1986). A translocated human c-myc oncogene is altered in a conserved coding sequence. *Proc. Natl. Acad. Sci. USA* **83**, 2939-2943.

Myung, J., Kim, K. B. and Crews, C. M. (2001). The ubiquitin-proteasome pathway and proteasome inhibitors. *Med. Res. Rev.* **21**, 245-273.

Palmer, A., Rivett, A. J., Thomson, S., Hendil, K. B., Butcher, G. W., Fuertes, G. and Knecht, E. (1996). Subpopulations of proteasomes in rat liver nuclei, microsomes and cytosol. *Biochem. J.* **316**, 401-407.

Pederson, T. (2001). Protein mobility within the nucleus–what are the right moves? *Cell* **104**, 635-638.

Pokrovskaja, K., Mattsson, K., Kashuba, E., Klein, G. and Szekely, L. (2001). Proteasome inhibitor induces nucleolar translocation of Epstein-Barr virus-encoded EBNA-5. *J. Gen. Virol.* **82**, 345-358.

Reits, E. A., Benham, A. M., Plougastel, B., Neefjes, J. and Trowsdale, J. (1997). Dynamics of proteasome distribution in living cells. *EMBO J.* **16**, 6087-6094.

Reyes, J. C. (2001). PML and COP1–two proteins with much in common. *Trends Biochem. Sci.* **26**, 18-20.

Salghetti, S. E., Kim, S. Y. and Tansey, W. P. (1999). Destruction of Myc by ubiquitin-mediated proteolysis: cancer-associated and transforming mutations stabilize Myc. *EMBO J.* **18**, 717-726.

Satou, A., Taira, T., Iguchi-Ariga, S. M. and Ariga, H. (2001). A novel transrepression pathway of c-Myc. Recruitment of a transcriptional corepressor complex to c-Myc by MM-1, a c-Myc-binding protein. *J. Biol. Chem.* **276**, 46562-46567.

Spencer, C. A. and Groudine, M. (1991). Control of c-myc regulation in normal and neoplastic cells. *Adv. Cancer. Res.* **56**, 1-48.

Stenoien, D. L., Patel, K., Mancini, M. G., Dutertre, M., Smith, C. L., O'Malley, B. W. and Mancini, M. A. (2001). FRAP reveals that mobility of oestrogen receptor-alpha is ligand- and proteasome-dependent. *Nat. Cell Biol.* **3**, 15-23.

Tao, W. and Levine, A. J. (1999). P19(ARF) stabilizes p53 by blocking nucleo-cytoplasmic shuttling of Mdm2. *Proc. Natl. Acad. Sci. USA* **96**, 6937-6941.

Wigley, W. C., Fabunmi, R. P., Lee, M. G., Marino, C. R., Muallem, S., DeMartino, G. N. and Thomas, P. J. (1999). Dynamic association of proteasomal machinery with the centrosome. *J. Cell Biol.* **145**, 481-490.

Visintin, R., Hwang, E. S. and Amon, A. (1999). Cfi1 prevents premature exit from mitosis by anchoring Cdc14 phosphatase in the nucleolus. *Nature* **398**, 818-823.

Wojcik, C., Schroeter, D., Wilk, S., Lamprecht, J. and Paweletz, N. (1996). Ubiquitin-mediated proteolysis centers in HeLa cells: indication from studies of an inhibitor of the chymotrypsin-like activity of the proteasome. *Eur. J. Cell Biol.* **71**, 311-318.

Xirodimas, D., Saville, M. K., Edling, C., Lane, D. P. and Lain, S. (2001). Different effects of p14ARF on the levels of ubiquitinated p53 and Mdm2 in vivo. *Oncogene* **20**, 4972-4983.

Yin, X., Landay, M. F., Han, W., Levitan, E. S., Watkins, S. C., Levenson, R. M., Farkas, D. L. and Prochownik, E. V. (2001). Dynamic in vivo interactions among Myc network members. *Oncogene* **20**, 4650-4664.